O. N. BABKINA, S. L. SARATOVSKIKH,
N. M. BRAVAYA
Laboratory of Catalysis of Polymerization Processes
Department of Polymer and Composite Materials
The Institute of Problems of Chemical Physics
Russian Academy of Sciences
142432 Chernogolovka, Moscow Region, Russia

Electroconductivity measurements in the solutions of catalytic systems based on metallocene complexes and various activators[*]

Summary — Electroconductivity (χ) was studied in 10^{-1} to 10^{-7} M bent-sandwich and ansa-metallocene (Cp_2 MX_2, $Me_2SiInd_2MX_2$, $Me_2SiCp_2MX_2$, Me_2SiCp-t-$BuMX_2$, $Me_2Si(2\text{-}MeInd)_2MX_2$, $(2\text{-}PhInd)_2MCl_2$, $EtInd_2ZrCl_2$ and $((cyclo\text{-}C_6H_{11})_2Cp)_2ZrCl_2$; M = Ti, Zr; X = Cl, Me) solutions (toluene, dimethylene chloride as varying polarity solvents) of homogeneous Ziegler—Natta catalyst systems derived *in situ* from the metallocene precursors and an organoaluminum compound ($AlEt_3$, $AlEt_2Cl$, Al-i-Bu_3), polymethylaluminoxane (MAO) or perfluorophenyl borate ($Ph_3CB(C_6F_5)_4$, $Me_2PhHNB(C_6F_5)_4$) as cocatalyst in relation to metallocene/activator ratio over a wide metallocene concentration range and in the absence or presence of an α-olefin. The specific electroconductivity of the reaction product solution was almost always higher than the sum of the electroconductivities of the individual component solutions measured under comparable conditions (Table 1). Apparent dissociation degrees and charged species equilibrium concentrations were evaluated (Tables 2, 3). The time profiles of electroconductivities and polymerization rates measured simultaneously were found to follow analogously descending courses (Figs. 3, 4). Low or very low metallocene concentration (10^{-5}—10^{-7} M), perfluorophenyl borate as activator, and sometimes also the α-olefin (propylene, hexene) added were found to enhance the electroconductivity (Table 1), *i.e.*, to favor the formation of charged species.

Key words: specific and equivalent electroconductivity, bent-sandwich and ansa-metallocenes, organoaluminum compounds, perfluorophenyl borates as cocatalysts.

This study adduces new evidence for the dissociative mechanism of formation of homogeneous metallocene-derived catalytic systems generated *in situ* from a titanocene or zirconocene precursor and an organoaluminum compound ($AlEt_3$, $AlEt_2Cl$, Al-i-Bu_3), polymethylaluminoxane (MAO), or perfluorophenyl borates ($Ph_3CB(C_6F_5)_4$, $Me_2PhHNB(C_6F_5)_4$) as cocatalyst. Electroconductivity was studied in 10^{-1}—10^{-7} M bent-sandwich and ansa-metallocene (Cp_2 MX_2, $Me_2SiInd_2MX_2$, $Me_2SiCp_2MX_2$, Me_2SiCp-t--$BuMX_2$, $Me_2Si(2\text{-}MeInd)_2MX_2$, $(2\text{-}PhInd)_2MCl_2$, $EtInd_2ZrCl_2$ and $((cyclo\text{-}C_6H_{11})_2Cp)_2ZrCl_2$ solutions (M = Ti, Zr; X = Cl, Me) containing a selected activator at varying metallocene/activator ratios, both in the absence and in the presence of olefin (propylene or 1-hexene), in media of various polarities (toluene, methylene chloride).

Each measurement was carried out in an electrolytic cell equipped with platinum electrodes. Measurements of the resistance of the reagents or reaction medium solutions examined were carried out over a wide range of concentrations. Specific and equivalent electroconductivities of the solutions studied were calculated according to the equations:

$$\chi = K\frac{1}{R} \tag{1}$$

$$\lambda = \frac{K \cdot 10^3}{RC} \tag{2}$$

where χ — *specific electroconductivity* ($\Omega^{-1} \cdot cm^{-1}$); λ — *equivalent electroconductivity* ($cm^2 \cdot \Omega^{-1} \cdot mol^{-1}$); R — *resistance*

---

[*] Presented at the 7th Seminar on "Organometallic Complexes as Catalysts of Vinyl Compounds Polymerization", Turawa n/Opole, 12—17 September 1999.

of solution (Ω); C — reagent solution concentration (mol/L) and K — cell's characteristic constant.

Comparative analysis of the conductivities of the dissolved individual "precursors" and of the corresponding complex catalytic systems confirms the occurrence of non-additive enhancement of specific conductivity when both the metallocene and the activator are present in the solution (Table 1). The major common observation for the systems studied is that the specific electro-conductivity (χ_{M+B+C}) of the reaction product solutions in various solvents and at all concentrations examined, is higher than the sum of the electroconductivities ($\chi_M + \chi_B + \chi_C$) of the individual component solutions measured under comparable conditions. This phenomenon is more pronounced in higher-polarity media (*cf.* Table 1: entries 3, 4; 7, 9; 31, 33) and at relatively lower metallocene concentrations; it depends on the nature of metallocene and activator. This effect indicates the formation

T a b l e 1. Comparison of specific electroconductivities[*] of various metallocene catalytic systems

Entry	Catalytic system	[M], mol/L	A/M, mol/mol	Solvent	[monomer], mol/L	$\dfrac{\chi_{M+B+C}}{\chi_M + \chi_B + \chi_C}$ [**]
1	Cp$_2$ZrCl$_2$/AlEt$_3$	2 · 10^{-6}	350	CH$_2$Cl$_2$		2.0
2	Cp$_2$ZrCl$_2$/AlEt$_2$Cl	1 · 10^{-1}	100	CH$_2$Cl$_2$		1.6
3	Cp$_2$ZrCl$_2$/MAO	1 · 10^{-1}	500	CH$_2$Cl$_2$		3.8
4	Cp$_2$ZrCl$_2$/MAO	1 · 10^{-1}	400	toluene		1.4
5	(2-PhInd)$_2$ZrCl$_2$/MAO	1 · 10^{-4}	1800	toluene		1.3
6	((*cyclo*-C$_6$H$_{11}$)$_2$Cp)$_2$ZrCl$_2$/MAO	3 · 10^{-5}	1700	CH$_2$Cl$_2$		3.1.
7	Me$_2$SiInd$_2$ZrCl$_2$/MAO	5 · 10^{-5}	1550	CH$_2$Cl$_2$		3.0
8	Me$_2$SiInd$_2$ZrCl$_2$/MAO/1-hexene	5 · 10^{-5}	1550	CH$_2$Cl$_2$	0.5	3.5
9	Me$_2$SiInd$_2$ZrCl$_2$/MAO	5 · 10^{-5}	1950	toluene		1.4
10	Me$_2$SiInd$_2$ZrCl$_2$/MAO/1-hexene	5 · 10^{-5}	1950	toluene	0.5	1.6
11	Me$_2$SiInd$_2$ZrCl$_2$/Al-*i*-Bu$_3$	2 · 10^{-5}	500	toluene		1.7
12	Me$_2$SiInd$_2$ZrMe$_2$/MAO	1 · 10^{-1}	100	CH$_2$Cl$_2$		4.6
13	Me$_2$SiInd$_2$ZrMe$_2$/MAO/1-hexene	1 · 10^{-1}	100	CH$_2$Cl$_2$	0.3	4.3
14	Me$_2$SiInd$_2$ZrMe$_2$/Me$_2$NHPhB(C$_6$F$_5$)$_4$	1 · 10^{-3}	1	CH$_2$Cl$_2$		1.0
15	Me$_2$SiInd$_2$ZrMe$_2$/Me$_2$NHPhB(C$_6$F$_5$)$_4$/1-hexene	1 · 10^{-3}	1	CH$_2$Cl$_2$	0.3	0.9
16	Me$_2$Si(2-MeInd)$_2$ZrMe$_2$/Me$_2$NHPhB(C$_6$F$_5$)$_4$	1 · 10^{-4}	1	toluene		1.3
17	NHPhB(C$_6$F$_5$)$_4$/1-hexene	1 · 10^{-4}	1	toluene	0.3	1.1
18	Me$_2$Si(2-MeInd)$_2$ZrMe$_2$/MAO	1 · 10^{-4}	2000	toluene		1.2
19	Me$_2$Si(2-MeInd)$_2$ZrMe$_2$/MAO/1-hexene	1 · 10^{-4}	2000	toluene	0.3	1.9
20	Me$_2$SiCp$_2$ZrMe$_2$/MAO	1 · 10^{-4}	2100	CH$_2$Cl$_2$		3.4
21	Me$_2$SiCp$_2$ZrMe$_2$/MAO/1-hexene	1 · 10^{-4}	2100	CH$_2$Cl$_2$		4.6
22	Me$_2$SiCp$_2$ZrMe$_2$/Me$_2$NHPhB(C$_6$F$_5$)$_4$	1 · 10^{-3}	1	CH$_2$Cl$_2$		1.0
23	Me$_2$SiCp$_2$ZrMe$_2$/Me$_2$NHPhB(C$_6$F$_5$)$_4$/1-hexene	1 · 10^{-3}	1	CH$_2$Cl$_2$	0.2	0.9
24	Me$_2$SiCp$_2$ZrMe$_2$/(CPh$_3$)(B(C$_6$F$_5$)$_4$)	1 · 10^{-3}	1	CH$_2$Cl$_2$		0.9
25	Me$_2$SiCp$_2$ZrMe$_2$/(CPh$_3$)(B(C$_6$F$_5$)$_4$)/1-hexene	1 · 10^{-3}	1	CH$_2$Cl$_2$	0.5	0.8
26	EtInd$_2$ZrMe$_2$/MAO	1 · 10^{-4}	1000	toluene		1.3
27	EtInd$_2$ZrMe$_2$/MAO/propylene	1 · 10^{-4}	1000	toluene	0.3	1.3
28	EtInd$_2$ZrMe$_2$/MAO	1 · 10^{-6}	1000	toluene		1.8
29	EtInd$_2$ZrMe$_2$/MAO/propylene	1 · 10^{-6}	1000	toluene	0.3	1.6
30	EtInd$_2$ZrCl$_2$/MAO	5 · 10^{-5}	2000	CH$_2$Cl$_2$		2.5
31	Me$_2$SiCp*N-*t*-BuTiMe$_2$/MAO	5 · 10^{-5}	2000	CH$_2$Cl$_2$		3.0
32	Me$_2$SiCp*N-*t*-BuTiMe$_2$/MAO/1-hexene	5 · 10^{-5}	2000	CH$_2$Cl$_2$	0.5	4.0
33	Me$_2$SiCp*N-*t*-BuTiMe$_2$/MAO	5 · 10^{-5}	2000	toluene		1.3
34	Me$_2$SiCp*N-*t*-BuTiMe$_2$/MAO/styrene	5 · 10^{-5}	2000	toluene	0.6	1.3
35	Me$_2$SiCp*N-*t*-BuTiMe$_2$/(CPh$_3$)(B(C$_6$F$_5$)$_4$)	5 · 10^{-5}	1	toluene		1.5
36	Me$_2$SiCp*N-*t*-BuTiMe$_2$/(CPh$_3$)(B(C$_6$F$_5$)$_4$)/1-hexene	5 · 10^{-5}	1	toluene	0.5	1.6

[*] Measured immediately after catalyst components were mixed. Specific electroconductivity *vs.* time resolved profiles in the absence of monomer will be reported elsewhere. For examples of changes with time in the presence of monomer, see Figs. 3, 4.

[**] χ_{M+B+C} — the specific electroconductivity of the metallocene/activator/monomer system, where: M — metallocene, B — activator, C — monomer; χ_M, χ_B, χ_C — the specific electroconductivities of metallocene, activator and monomer, resp.

of the products endowed with higher electroconductivities than those of the starting reagents in the course of catalyst component interactions. The higher the effect, the higher the discrepancy between (χ_{M+B+C}) and $\chi_M + \chi_B + \chi_C$. The effect is manifest in each catalytic system examined here.

The ionic species forming when the catalyst components interact with each other increase the specific electroconductivities of the reaction mixture solutions as compared with those of the individual components. Comparison of the action of aluminum alkyls (or halide alkyls) with that of MAO shows that, when used as medium, the more polar solvent MAO generated charged species more effectively than the former compounds did (cf. Table 1: entries 1, 2, 3), whereas in toluene as solvent, the ability to generate charged species is similar (entries 9, 11) at least at the experimental concentrations of the metallocene. At a metallocene concentration of about $1 \cdot 10^{-4}$ mol/L and at similar Al/Zr ratios, different metallocenes showed related specific electroconductivities (entries 5, 18). However, as shown below, a decrease in metallocene concentration gives rise to an enhanced efficiency to form charged species; the effect of the metallocene structure becomes more pronounced at rather low concentrations. With perfluorophenyl borate as activator, the related specific electroconductivity is also seen to increase (entries 33, 35). Again, upon addition of an olefin, the specific electroconductivity rose considerably (cf. Table 1: entries 18, 19; 20, 21). In some cases, a fast conversion of the α-olefin accompanying deactivation of active species prevented an increase in electroconductivity.

For some catalytic systems, apparent dissociation constants and charged species equilibrium concentration were calculated. The relationship between equivalent electroconductivity and metallocene concentration is described by the empirical equation:

$$\lambda = \lambda_\infty - A\sqrt{C} \qquad (3)$$

The equivalent electroconductivities measured within the range of low concentrations allowed to evaluate λ_∞
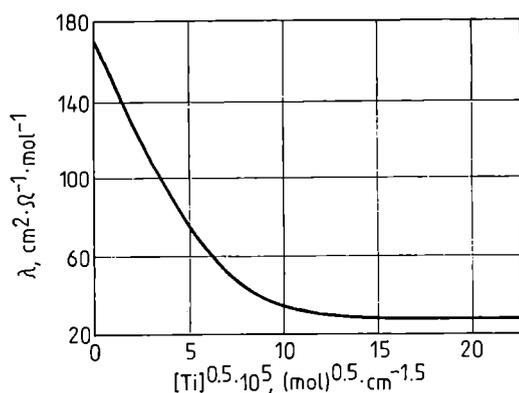

Fig. 1. Equivalent electroconductivity of $Me_2Si[(CH_3)_4Cp]N$-t-$BuTiMe_2/MAO$ solution in CH_2Cl_2 in relation to titanium complex concentration at room temperature

(i.e., equivalent electroconductivity obtained by extrapolation of $\lambda_\infty/[Ti]^{0.5}$ to "zero" concentration of metallocene, Fig. 1) and thus to calculate the dissociation degree ($\alpha = \lambda_c/\lambda_\infty$) as a measure of cationic species formation while catalyst components interact with each other. Results are presented in Tables 2 and 3. One can see that, at all the examined Al/M ratios, the concentration of ionic species increased as the metallocene concentration was decreased. From our observations, dissociation degrees α approach values of 50% or even higher when the content of a metallocene is as low as 10^{-6} M. Thus, it equals 16% at a titanium precursor concentration of $5.4 \cdot 10^{-5}$ mol/L and 63% at [Ti] = $1.0 \cdot 10^{-6}$ mol/L in a methylene chloride solution of $Me_2SiCp*N$-t-$BuTiMe_2/MAO$

Table 2. Electroconductivity parameters of the $Me_2SiCp*N$-t-$BuTiMe_2/MAO$ catalytic system in CH_2Cl_2 as solvent; Al/Ti (mol/mol) = 2000

[Ti], mol/L	λ_{Ti}, cm$^2 \cdot \Omega^{-1} \cdot$ mol^{-1}	α	[Ti$^+$], mol/L
$5.4 \cdot 10^{-5}$	28.04	0.16	$8.64 \cdot 10^{-6}$
$1.0 \cdot 10^{-6}$	107.15	0.63	$6.30 \cdot 10^{-7}$
$5.0 \cdot 10^{-7}$	125.61	0.73	$3.65 \cdot 10^{-7}$
	λ_∞ = 171.05		

Table 3. The electroconductivities of $Cp_2ZrCl_2/AlEt_2Cl$ solutions in methylene dichloride and ionic species concentration in relation to metallocene concentration at varying Al/Zr ratios

Al/Zr	[Zr], mol/L	λ, cm$^2 \cdot \Omega^{-1} \cdot$ mol^{-1}	α	[Zr$^+$] mol/L	[Zr$^+$], %
50	$1,0 \cdot 10^{-4}$	0.88	$4.89 \cdot 10^{-3}$	$4.89 \cdot 10^{-7}$	0.5
	$5.0 \cdot 10^{-5}$	0.13	$6.49 \cdot 10^{-4}$	$3.47 \cdot 10^{-8}$	0.1
	$1.0 \cdot 10^{-5}$	2.24	$1.24 \cdot 10^{-2}$	$1.24 \cdot 10^{-7}$	1.2
	$5.1 \cdot 10^{-6}$	2.19	$1.22 \cdot 10^{-2}$	$6.22 \cdot 10^{-8}$	1.2
	$1.1 \cdot 10^{-6}$	37.04	0.21	$2.22 \cdot 10^{-7}$	20.6
	0	$180.00 = \lambda_\infty$			
100	$9.0 \cdot 10^{-5}$	1.69	$6.53 \cdot 10^{-3}$	$5.88 \cdot 10^{-7}$	0.65
	$5.0 \cdot 10^{-5}$	0.46	$1.74 \cdot 10^{-3}$	$8.69 \cdot 10^{-8}$	0.20
	$1.0 \cdot 10^{-5}$	2.62	$1.01 \cdot 10^{-2}$	$1.01 \cdot 10^{-7}$	1.01
	$5.0 \cdot 10^{-6}$	2.73	$1.05 \cdot 10^{-2}$	$5.28 \cdot 10^{-8}$	1.05
	$1.1 \cdot 10^{-6}$	12.35	$4.77 \cdot 10^{-2}$	$5.15 \cdot 10^{-8}$	4.80
	$5.5 \cdot 10^{-7}$	83.73	0.32	$1.76 \cdot 10^{-7}$	32.30
	0	$258.78 = \lambda_\infty$			
500	$5.0 \cdot 10^{-5}$	0.92	$1.91 \cdot 10^{-2}$	$9.54 \cdot 10^{-7}$	1.9
	$9.8 \cdot 10^{-6}$	4.89	0.10	$9.94 \cdot 10^{-7}$	10.1
	$1.0 \cdot 10^{-6}$	29.58	0.61	$6.38 \cdot 10^{-7}$	61.4
	$5.4 \cdot 10^{-7}$	34.84	0.72	$3.87 \cdot 10^{-7}$	72.3
	0	$48.19 = \lambda_\infty$			
1000	$5.0 \cdot 10^{-5}$	2.83	$2.19 \cdot 10^{-2}$	$1.09 \cdot 10^{-6}$	2.2
	$9.4 \cdot 10^{-6}$	12.39	$9.58 \cdot 10^{-2}$	$9.00 \cdot 10^{-7}$	9.6
	$1.0 \cdot 10^{-6}$	29.81	0.23	$2.40 \cdot 10^{-7}$	23.0
	$5.2 \cdot 10^{-7}$	58.70	0.45	$2.38 \cdot 10^{-7}$	45.4
	0	$129.38 = \lambda_\infty$			
2000	$1.0 \cdot 10^{-6}$	31.33	0.12	$1.25 \cdot 10^{-7}$	12.2
	$5.0 \cdot 10^{-7}$	99.21	0.39	$1.94 \cdot 10^{-7}$	38.6
	0	$257.20 = \lambda_\infty$			

at Al/Zr = 2000 (Table 2). A similar tendency of increasing the dissociation degree with a decrease in zirconocene concentration was revealed in a methylene chloride solution of the $Cp_2ZrCl_2/AlEt_2Cl$ system (Table 3). However, the Al/Zr ratio is also a factor very important for the dissociation process. Thus, at low metallocene
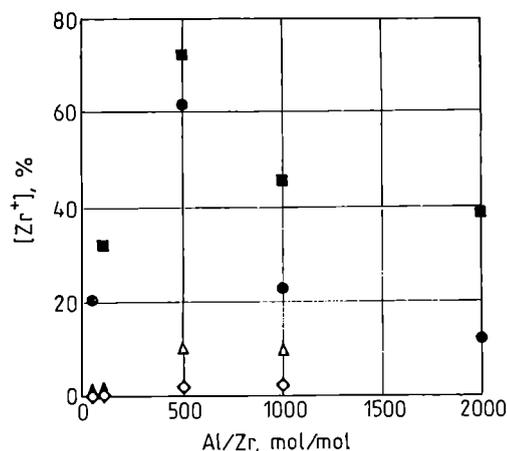

Fig. 2. Ionic species concentration in relation to Al/Zr ratio at varying metallocene concentrations for $Cp_2ZrCl_2/AlEt_2Cl$ catalytic system in CH_2Cl_2 as solvent; [Zr] = 5 · 10^7 (■); 1 · 10^{-6} (●); 1 · 10^{-5} (△); 5 · 10^{-5} mol/L (◇)
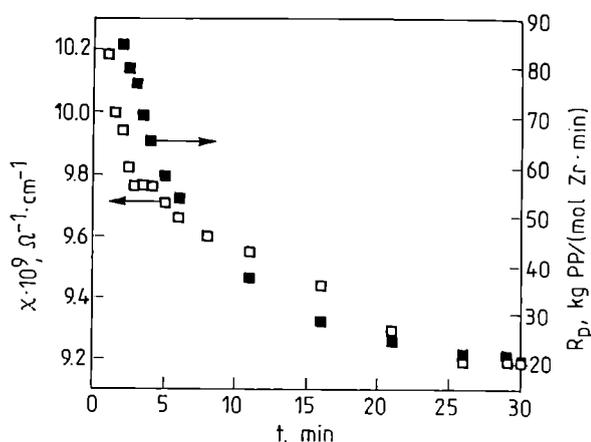
Fig. 3. Specific electroconductivity vs. time (left ordinate) and propylene polymerization rate vs. time (right ordinate) profiles for simultaneous measurements in the course of propylene polymerization catalyzed by the $EtInd_2ZrMe_2/MAO$ system; polymerization conditions: toluene, $30^\circ C$, [Zr] = 2.0 · 10^{-5} mol/L, Al/Zr = 1000 (for symbols see Fig. 2)

concentrations we observed a bell-like dependence of ionic species concentration on Al/Zr ratio, reaching a maximum at Al/Zr = 500 (Fig. 2). At higher metallocene concentrations the effect was less pronouced.

Simultaneous measurements of electroconductivity and

olefin consumption rate in the course of the reaction were carried out for a series of catalytic systems. To illustrate the pattern, the propylene consumption kinetics is presented together with changes in electroconductivity for the $EtInd_2ZrMe_2/MAO$ and $EtInd_2ZrMe_2/Me_2NHPhB(C_6F_5)_4$ catalytic systems in toluene as solvent (Figs. 3, 4). This zirconocene is useful for comparison because it demonstrates a moderate activity in propylene polymerization and does not give rise to fast formation of a great amount of the precipitating polymer. Figures 3—4 show the propylene
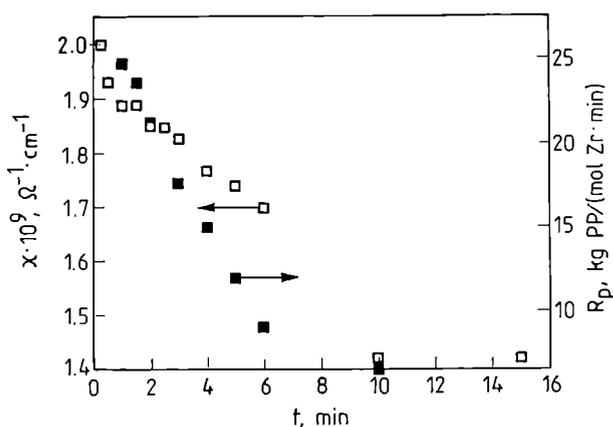

Fig. 4. Specific electroconductivity vs. time (left ordinate) and propylene polymerization rate vs. time (right ordinate) profiles for simultaneous measurements in the course of propylene polymerization catalyzed by the $EtInd_2ZrMe_2/Me_2NHPhB(C_6F_5)_4$ system; polymerization conditions: toluene, $40^\circ C$, [Zr] = 9.2 · 10^{-5} mol/L, Zr/B = 1 (for symbols see Fig. 2)

consumption rate vs. time and electroconductivity vs. time profiles to follow similar descending courses. Upon addition of α-olefin to the non-polymerizing system ($Cp_2ZrCl_2/MAO/1$-hexene) the specific electroconductivity decreased but slightly and then remained unchanged as reported earlier [1]. The present comparison is only qualitative. A more precise analysis and dissociation degree measurements could provide a quantitative characteristics of each catalytic system examined. The present experiments demonstrate the relevance of ionic species to the key intermediates in polymerization catalysis.

REFERENCES

1. Babkina O. N., Bravaya N. M., Dyachkovskii F. S.: Polimery 1997, 42, 630.